Optics and Lasers in Engineering 47 (2009) 1028–1033

Contents lists available at ScienceDirect

Optics and Lasers in Engineering

journal homepage: www.elsevier.com/locate/optlaseng

A novel time-division multiplexing fiber Bragg grating sensor interrogator for structural health monitoring

Yongbo Dai [a], Yanju Liu [b], Jinsong Leng [c,*], Gang Deng [b], Anand Asundi [d]

[a] Department of Automatic Test and Control, No. 92 West DaZhi Street, Harbin Institute of Technology (HIT), Harbin 150001, PR China
[b] Department of Aerospace Science and Mechanics, No. 92 West DaZhi Street, Harbin Institute of Technology (HIT), Harbin 150001, PR China
[c] Centre for Composite Materials, No. 2 YiKuang Street, Science Park of Harbin Institute of Technology, P.O. Box 3011, Harbin 150080, PR China
[d] School of Mechanical and Aerospace Engineering, Nanyang Technological University, Singapore

ARTICLE INFO

Available online 26 June 2009

Keywords:
Fiber Bragg grating sensor
Wavelength-division multiplexing
Time-division multiplexing
Structural health monitoring

ABSTRACT

A novel fiber Bragg grating (FBG) sensor system for measurement of strain and temperature is proposed in this paper. The proposed sensor technique is based on time-division multiplexing (TDM). A semiconductor optical amplifier (SOA), connected in a ring cavity, is used to serve as a gain medium and switch. The SOA is driven by a pulse generator, which operates the SOA at different periods of time to select reflected pulses from a particular sensor. The FBG sensors have identical center wavelengths and can be deployed along the same fiber. This technique relieves the spectral bandwidth issue and permits the interrogation of up to 100 FBGs along a fiber, if the reflectivity of the individual sensors is sufficiently low to avoid shadowing effects. This system is particularly suitable for the application in structural health monitoring (SHM) where large numbers of sensors are required in wide measurement ranges.

1. Introduction

Fiber Bragg grating (FBG) sensors are ideally suited for structural health monitoring of composite materials and concrete structures [1–5]. Among the different multiplexing techniques of FBG sensors, the wavelength-division multiplexing (WDM) technique is one of the most widely used [6]. The maximum number of multiplexed sensors are limited by the width of the broadband (or wavelength-scanned) light source and by the Bragg wavelength operation ranges required by the FBG sensors. The WDM systems commonly operate in a continuous-wave mode that requires each sensor to occupy a distinct wavelength window. Typically, for a strain measurement system with a range of 10,000 με and using an optical source with 50 nm bandwidth at 1550 nm, the maximum number of sensors is five per fiber [7]. However, in many structural health monitoring applications, multiplexing of more than five sensors is required along a single fiber. Furthermore, a high degree of multiplexing enables reduction in both cost and complexity in a multipoint configuration and increases the competitiveness of these sensors against conventional electrical sensors. An alternative technique is the time-division multiplexing (TDM) technique, where a pulsed source is used to illuminate the gratings placed at different distances from the source [7,8]. The reflected signals from the gratings are separated in time domain. If each FBG sensor occupies the same wavelength window, then the total number of sensors does not depend on the bandwidth of the source. All the FBG sensors use the same wavelength range, and the interrogation unit receives a number of reflection pulses from each grating. These pulses arrive at a time determined by the distance between interrogator and FBG sensor, and one FBG sensor can be distinguished from another by analyzing the pulse arrival times [8]. This design results in lower cost and allows up to 100 strain or temperature sensors to be incorporated into a single channel system. Consequently, this TDM system allows measuring many more FBG sensor points per fiber than a conventional WDM system, combined with lower system cost [9–11].

2. Principle

The typical TDM configuration is illustrated in Fig. 1 [12,13]. The light source generates a short optical pulse. When the pulse is transmitted in the FBG array, each of the FBG sensors at distances L_i from the light source will reflect a small part of the pulse, and the reflected parts enter into the optical switch via the coupler.

The reflected pulses arrive at the optical switch with delays of

$$\tau_i = 2nL_i/c \quad (1)$$

* Corresponding author. Tel./fax: +86 451 86402328.
E-mail address: lengjs@hit.edu.cn (J. Leng).

0143-8166/$ - see front matter Crown Copyright © 2009 Published by Elsevier Ltd. All rights reserved.
doi:10.1016/j.optlaseng.2009.05.012

n is the effective refractive index of optical fiber and c the light velocity in vacuum.

Delay time of the optical switch can be adjusted to one of the FBG sensors, and the reflection spectrum of this particular FBG sensor is measured by the CCD detector. So by changing the delay time any one of the reflected spectra of the FBG array can be interrogated. However, the interval between the reflected pulses can become very short for dense sensor arrays, and the speed of the electro-optic switch may not be able to match this.

An alternative to electrical gating is optical gating: an optical modulator is used to transmit and amplify only reflections for a single grating in the array. Reflections from the isolated grating may be integrated over time and the wavelength can be extracted.

The TDM system based on optical gating uses a semiconductor optical amplifier (SOA) as shown in Fig. 2. Typically, a SOA is used in a continuously-on mode as an amplifier in telecommunications networks. Here, in the TDM interrogation design, it is driven by a programmable pulse generator in a short, high-power-pulsed configuration. When the SOA is first enabled, the drive circuit causes the SOA to emit a short broadband optical pulse through the generation of amplified spontaneous emission (ASE). Thus, the SOA is used as the only light source. The generated broadband pulse propagates towards the FBG sensor array via the fiber reel L to the FBG sensors at distances L_i. When the pulse arrives at each sensor, a small reflection begins propagating back towards the SOA.

At time τ_i (see Eq. (1)), when the reflection from an individual FBG sensor arrives at the SOA, the drive circuit switches on the SOA again. The weakly reflected signal passes through the SOA and is amplified. The amplified signal passes through the isolator and is measured by the optical spectrum analyzer (OSA), the sensor data can be read out. The delay τ_i of the generator can be varied, and any FBG sensor in the array can be read out. The SOA can work in a high-speed switch mode with minimum switch time of 1 ns.

The operating principle of the switch is illustrated in Fig. 3a. First electrical drive pulse is applied to the SOA and an optical broadband pulse P is generated and launched into the fiber sensor array. At time T1, part of the optical pulse P is reflected by the grating G1 with a spectral pulse of Bragg wavelength $\lambda 1$ towards the SOA. The remainder of the optical pulse P will continue towards the other gratings. At time 2T1, a second electrical drive pulse is applied to the SOA, causing a second optical pulse P to be generated and launched into the fiber. At the same time, the first reflected pulse $\lambda 1$ arrives back at the SOA. Since the SOA is switched on, it will be transmitted and amplified as described above. The first reflected pulse $\lambda 1$ will then propagate to the OSA. However, at this same time, the remainder of the first optical pulse P will arrive at the grating G2, where a part of it will be reflected, creating a second reflected spectral pulse at Bragg wavelength $\lambda 2$. From time 2T1 to 2T1+2Ts, the $\lambda 1$ and $\lambda 2$ pulses will arrive at the SOA in same order. The on time of the SOA is T_w and the interval between the optical pulses $\lambda 1$ and $\lambda 2$ is 2Ts.

If the width T_w of the pulses is more than the interval 2Ts, like the red inset in Fig. 3b, then the OSA cannot distinguish $\lambda 1$ from $\lambda 2$. So, in this TDM system, the width of the pulses should be less than the minimal time interval between two neighbored sensors.

From the linear arrangement in Fig. 3a, a novel ring cavity configuration has been derived that forms the basis for the interrogator as illustrated in Fig. 4. The optical loop includes a fiber reel L1, an array of low-reflectivity FBG sensors which have identical mean resonant wavelength, a ring cavity which is comprised of a semiconductor optical amplifier and couplers 1 and 2. A pulse generator provides a stream of pulses of programmable period and duration to drive the SOA. When the electrical drive circuit turns on and causes the SOA to generate a short broadband optical pulse which emit via the port 1 and 2 of the SOA. The fiber reel L1 has a proper length and the optical pulses emitted from port 1 and 2 arrive at the coupler 2 at the same time, then the two optical pulse form a more

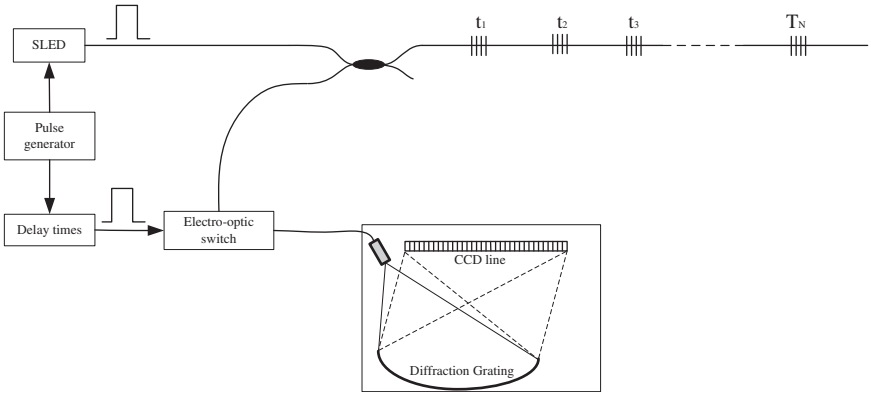

Fig. 1. Typical combined TDM/WDM FBG interrogator with electro-optic grating [12,13].

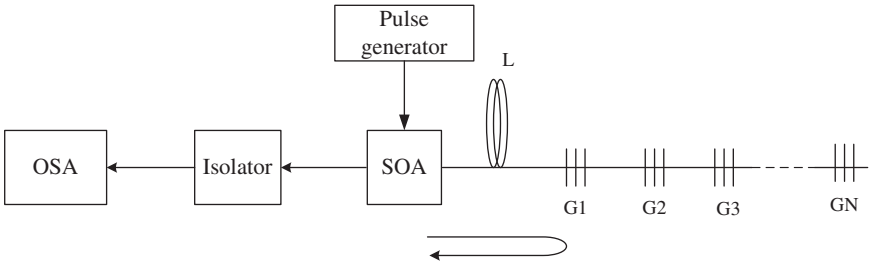

Fig. 2. Scheme of switched SOA-based TDM FBG interrogator.

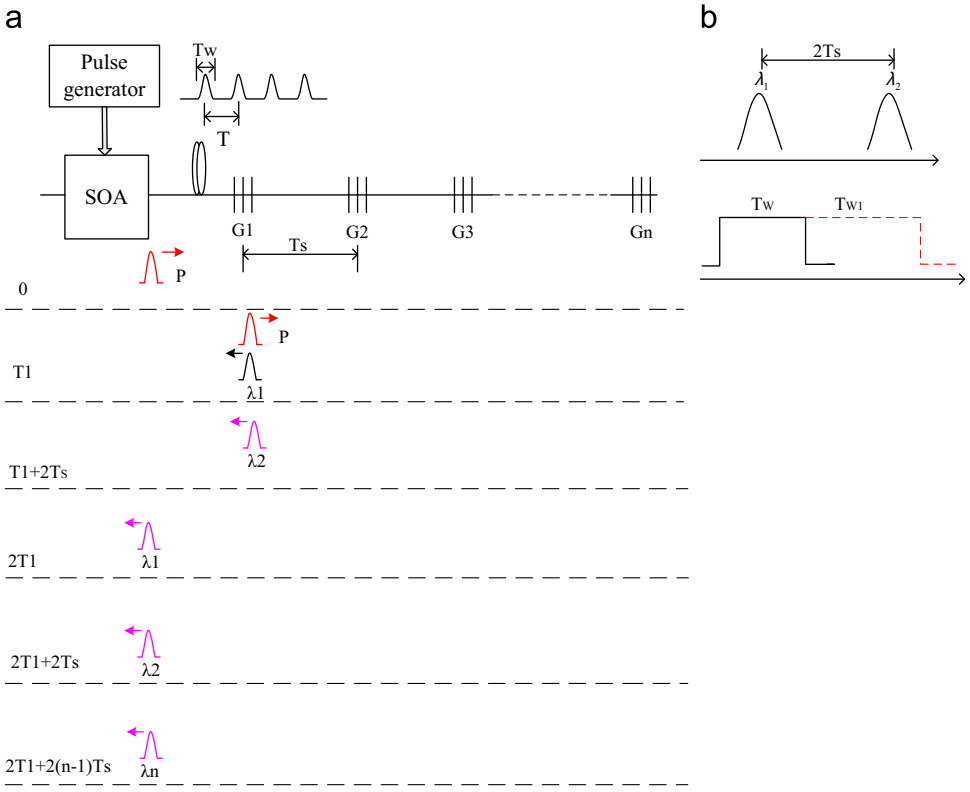

Fig. 3. (a) Time/position scheme of light pulses emitted from a pulsed SOA and (b) the limit of pulse width in the TDM system of (a).

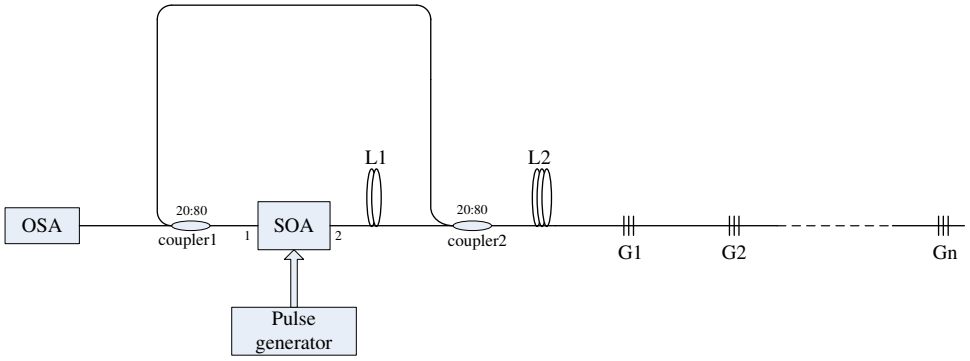

Fig. 4. Switched-SOA-based ring cavity FBG TDM configuration.

stronger optical pulse and enter the FBG sensor array through the coupler 2.

On reaching each grating, part of the pulses will be reflected, the reflected pulses arrive at the coupler 2 and are split into two parts: 80% of the pulse arrives at port 2 of the SOA, and the remainder arrives at port 1 of the SOA. When the SOA is switched on, the incoming pulses will pass through and be amplified by over 15 dB, while the other pulses will be absorbed, when the SOA is switched off. So, we may tune the period of the driving pulse to equal the round-trip time between the SOA and the FBG. The fiber reel length L2 (larger than the distances between FBG sensors) ensures that only one set of reflected signals can propagate in the cavity at one time, and the round-trip time of any sensor in the array is not an integer multiple of another sensor.

Each of the FBG sensors can be addressed by different periods of the SOA driving pulse, and unlike the WDM systems this system does not address the sensors by their mean Bragg wavelength.

If the length difference ΔL of fibers from the two ports of the SOA to coupler 2 is large, the pulses emitted from the two ports of the SOA arrive at the coupler 2 at different times ($\Delta L = 1$ m produce a pulse delay of 5 ns). In the experiment, the length difference from the two ports to the coupler 2 is much smaller than 1 m and the width of the pulses is 40 ns, so the delay between the two pulses remains <1 ns and can be neglected.

An example for measuring the particular sensor G_i is used to illustrate how the TDM FBG interrogator works.

When the SOA is first activated by the pulse generator, the generated ASE pulse simultaneously emits from the two ports of the SOA, which add together at coupler 2 and propagate towards the FBG sensor array. After time T_i, which is equal to the round-trip time between the sensor G_i and the SOA, the pulse λ_i reflected by sensor G_i is split into λ_{i1} and λ_{i2} by coupler 2 and arrives simultaneously at the SOA. The pulse generator switches the SOA on again, allowing λ_{i1} and λ_{i2} to pass be amplified.

Because the total power of the SOA is constant and has the input signals λ_{i1} and λ_{i2}, the optical pulse emitted from the two ports of the SOA includes broadband ASE background and the amplified narrow sensor signal. The SOA is driven at the period of T_i, the pulse λ_i reflected by sensor G_i will travel through the SOA repeatedly, and the power of signal λ_i will increase and the ASE background will decrease. After approximately five cycles, the system reaches equilibrium. The loss in the cavity equals the gain provided by the SOA. After this short time (typically a few μs), the optical signal in the cavity will consist largely of a narrow band peak. The output signal leaving the ring cavity contains only a single sensor signal and can be extracted using a wavelength demodulator.

Changing the time T_i and repeating the above process, the system can measure any of the FBG sensors along the fiber.

3. Estimation of error signal caused by multiple reflections

When the reflected pulse propagates towards the SOA, part of it can be reflected by FBGs of same Bragg wavelength. Fig. 5 shows the multiple reflections at the FBGs. Such multiple reflections may cause cross talk. Assuming the reflectivity of FBG is constant, a and the power of the source is unity, the reflected pulses by G1, G2, and G3 are shown in Eq. (2)

$$P_1 = a$$
$$P_2 = a(1-a)^2$$
$$P_3 = a(1-a)^4 \quad (2)$$

The reflected pulse P_2 will be partially reflected by G1 and reflected again by G2 to form pulse P_{21}. Fig. 5 shows that the P_3 and P_{21} will arrive at the SOA at the same time. The signals P_3 and P_{21} may be described by the following equations:

$$P_{21} = a^3(1-a)^2$$
$$P_3/P_{21} = (1-a)^2/a^2 \quad (3)$$

Consider a numerical example, assuming an upper limit for reflectivity $a = 5\%$. Then we obtain the relation $P_3/P_{21} = 361$, i.e., P_3 is much higher than P_{21}, and hence P_{21} can be neglected. Using low-reflectivity FBGs is necessary for multiplexing a high number of sensors to avoid multiple reflection interference.

The reflected power of the FBG at different reflectivity and number of sensors is shown in Fig. 6. Based on Eq. (2), we can get the formula

$$P_n = a(1-a)^{2(n-1)} \quad (4)$$

Eq. (4) indicates that the power can be changed by the reflectivity and the number of the sensors. Fig. 6 shows the relation between the power and the number of the sensors for five different reflectivities, illustrating a decrease in power with increasing number of the sensors. The power decreases sharply at a reflectivity of 0.05 (higher shadowing) and slowly at a reflectivity of 0.01. Using 100 sensors, the power almost decrease to zero at a reflectivity of 0.05, while the power is still enough to be measured at a reflectivity of 0.01. Beside such simple power balance, stronger limitations exist by partly shadowing of

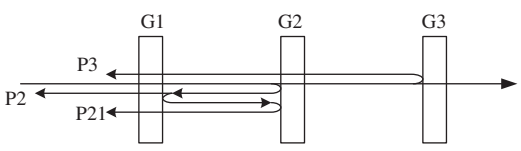

Fig. 5. Multiple reflections at FBG sensors of (almost) equal Bragg wavelength.

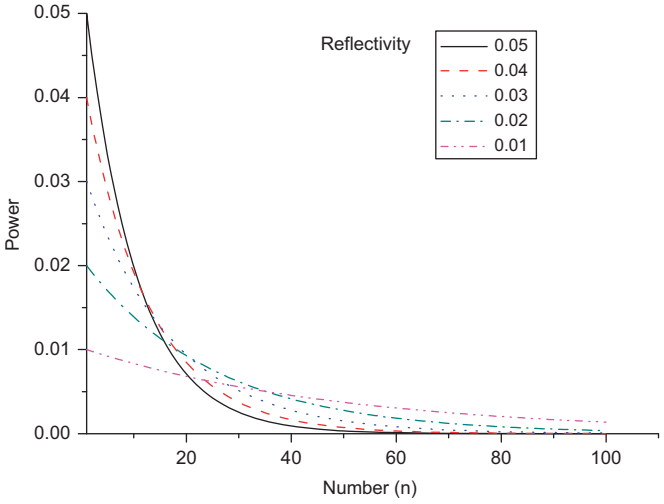

Fig. 6. Reflected power of large number of sensors at different reflectivity.

sensor spectra, with consequent deformation of the received spectrum and erroneous results of Bragg wavelength measurement. For 100 FBG sensors, maximum reflectivity should be 0.04 [9]. Consequently, low reflectivity of the FBG sensors is necessary for the TDM system.

4. Experiments

The experimental device used to evaluate the ring cavity approach is shown in Fig. 7. Three sensors were put into beaker filled by water and the temperature difference was monitored using the TDM system. The SOA was driven by the programmable pulse generator circuit, the Agilent 33220A that uses a direct digital synthesis (DDS) technology to accurately tune the frequency and width of the pulse. The fiber reel L2 consisted of approximately 2000 m of single mode telecommunications fiber, providing a 9780 ns delay for optical pulse. The system was tested with an array of 3 FBGs having nearly identical Bragg wavelengths of 1550 nm and reflectivity of 5%, the length of the fiber LD is 5 m and is used to separate each FBG. To evaluate the level of sensor isolation, the wavelength of each grating was partially offset by using different temperature water, based on the FBG knowledge, the wavelength of G1, G2, and G3 is different, we can distinguish the position of the grating by the shift of wavelength.

The length of the fiber L2 is 2000 m and the round-trip time between the SOA and the first FBG is 19.56 μs, so the frequency of the pulse generator should be close to 51 kHz. The time interval of the reflected optical pulses by the FBGs is 50 ns and the width of the drive pulse is set to 40 ns to separate each reflected optical pulse. In this experiment, taking into account that the gratings have an identical central wavelength, the FBGs were placed in ranging in temperatures from 40 °C (hot water), to 20 °C (normal water), and to 0 °C (ice water), respectively. We reduce the frequency gradually from 51 to 50.11, 49.99, 49.87 kHz, to sequentially address gratings G1,G2, and G3, respectively. Fig. 8 shows the recordings taken using the OSA when the pulse generator was sequentially adjusted to address the 3 FBGs in turn. Because of difference in water temperature, the central wavelength shows an obvious shift, but no measurable cross talk. The results show that the FBG sensors provide an extremely repeatable signal profile with a peak power of −46 dBm, a background level of −66 dBm, and an optical signal-to-background-noise level of 20 dB. In reference [8], the author's

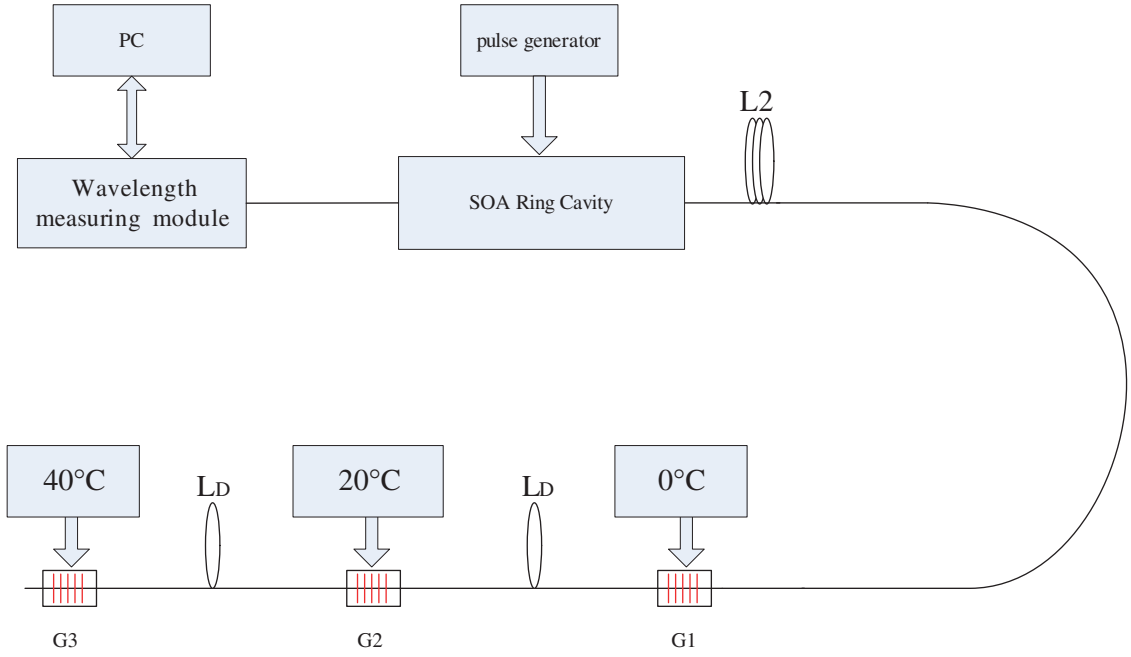

Fig. 7. Experimental TDM interrogator of 3 FBG sensors.

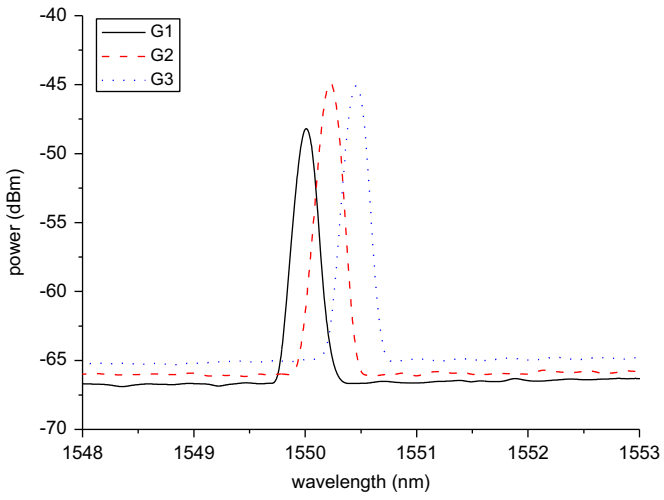

Fig. 8. Optical spectra obtained from 3 FBGs G1…G3, kept at different temperatures 0, 20, and 40 °C, respectively.

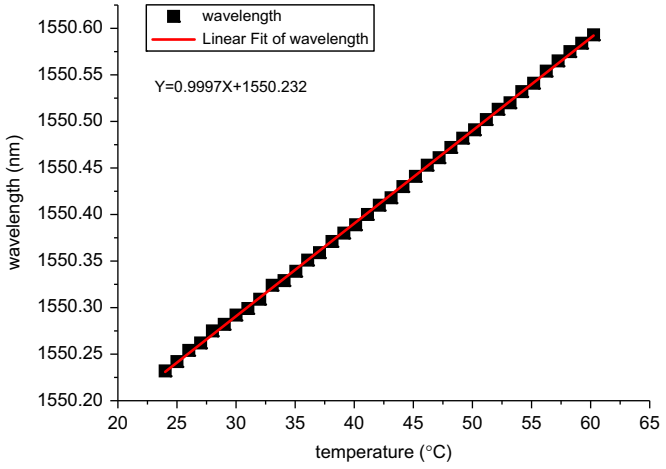

Fig. 9. Temperature characteristic of the Bragg wavelength, with slope of 10.0 pm/K at mean Bragg wavelength of 1550.4 nm.

system can obtain high-quality signal with an average power of −24 dBm, because of the length of the optical fiber is 220 m and the operating frequency of SOA is near 1 MHz, in this experiment the operating frequency of SOA is near 50 kHz, so in the same time the current system measures fewer pulses and the average power is lower.

The data we measured is average power but not instantaneous power, the signal-to-background-noise level is 30 dB. These levels of performance are excellent for the TDM system.

In order to evaluate the linearity of the TDM system, FBG2 was placed in a beaker of water whose temperature varied from 24 to 60 °C and measured using a temperature sensor. The temperature increase results in a wavelength change from 1550.232 to 1550.593 nm. The results shown in Fig. 9 indicate a good linear relationship between wavelength and temperature, with a coefficient of 10.0 pm/°C. This result agrees with the thermo-optic coefficient of the fiber. This experiment shows than the interrogator has good linearity and the precision is comparable to the WDM system.

5. Conclusions

We have demonstrated a novel FBG sensor system based on ring cavity configuration using TDM to demultiplex up to 100 FBGs in one fiber. The ring cavity configuration can capture and amplify the weak sensor signal so that the demodulator can measure FBGs with low reflectivity. Estimations show negligible cross talk. The low component count and low loss features of the system improve the power and extinction ratio of the sensing signals significant. This system is ideal for implementing large

numbers of FBG sensors for structural health monitoring (SHM) applications.

References

[1] Leng JS, Asundi A. Structural health monitoring of smart composite materials by using the extrinsic Fabry–Perot interferometer and fiber Bragg grating sensors. Sensors and Actuators A 2003;103:330–40.

[2] Leng JS, Asundi A. Real-time cure monitoring of smart composite materials using extrinsic Fabry–Perot interferometer and fibre Bragg grating sensors. Smart Materials and Structures 2002;11:249–55.

[3] Merzbacher CI, Kersey AD, Friebele EJ. Fibre optic sensors in concrete structures: a review. Smart materials and structures 1996;5:196–208.

[4] Leng JS, et al. Structural NDE of concrete structures using protected EFPI and FBG Sensors. Sensors and Actuator A 2006;l26:340–7.

[5] Leng JS, et al. Structural health monitoring of concrete cylinder using protected fibre optic sensors. Smart Materials and Structures 2006;15(2):302–8.

[6] Berkoff TA, Davis MA, Bellemore DG, Kersey AD, Williams GM, Putnam MA. Hybrid time and wavelength-division multiplexed fibre grating array. Proc SPIE 1995;2444:288–90.

[7] Lloyd GD, Everall LA, Sugden K, Bennion I. Resonant cavity time-division-multiplexed fiber Bragg grating sensor interrogator. IEEE Photon Technol Lett 2004;16(10):2323–5 (October 2004).

[8] Chung WH, Tam HY, Wai PKA, Khandelwal A. Time- and wavelength-division multiplexing of FBG sensors using a semiconductor optical amplifier in ring cavity configuration. IEEE Photon Technol Lett 2005;17(12):2709–11 (December 2005).

[9] Cooper DJ, Coroy T, Smith PWE. Time-division multiplexing of large serial fiber-optic Bragg grating sensor arrays. Appl Opt 2001;40:2643–54.

[10] Lloyd GD, Everall Lorna A, Sugden Kate, Bennion Ian. A high-performance miniaturized time-division multiplexed sensor system for remote structural health monitoring. Proc SPIE 2004;5459:145–55.

[11] Lloyd GD, Bennion I, Everall LA, Sugden K, Novel resonant cavity TDM demodulation scheme for FBG sensing. In: Proc CLEO, San Francisco, CA, Paper CWD4, May 2004.

[12] Askins CG, Putnam MA, Optical spectrometer with improved geometry and data processing for monitoring fiber optic Bragg gratings, US patent 6,233,373, 2001.

[13] Ecke W, Nunes LCS, Valente LCG, Schroeder K, Chojetzki C, Willsch R, OTDR Multiplexed High-Birefringent Fiber Grating Sensor Network for Transversal Strain and Optochemical Monitoring. In: Proc. sixteenth int conf opt Fiber Sensors, IEICE Japan, ISBN 4-89114-036-4, 2003 pp. 548–551.